Chapter 4

Stress intensity in a thermoroll

D. Beder[1], T. Myers[2], J. Ockendon[3] A. Peirce[4], B. Van Fliert[5], M. Ward[6]

written by Michael J. Ward

1 Introduction

This report describes the mathematical results obtained by a team of researchers working at the 1997 PIMSIPS Workshop investigating the stress buildup and temperature profiles in a thermoroll. The problem under consideration was brought to the workshop by Dr. Roman Popil of MacMillan Bloedel Research representing MacMillan Bloedel Ltd. The problem description provided, including the background, questions, and data are given below in §1, §2 and Appendix A.

The outline of the report is as follows. In §3 we give some physical estimates. In §4 and §5 we model the temperature field in the thermoroll in two different regions of the roll and we calculate the corresponding temperature gradient. In §6 we estimate the stress induced by the temperature gradients in order to determine the location of the maximum stress and to determine any possible singular behavior of the stress field. Such a singular behavior could lead to the formation of cracks. Finally, in §7 we state our conclusions.

[1] Dept. of Physics, UBC, Vancouver
[2] Dept. of Mathematics, Cranfield Institute, U.K.
[3] Dept. of Mathematics, Oxford University, U.K.
[4] Dept. of Mathematics, UBC, Vancouver
[5] Dept. of Mathematics, Leiden University, Netherlands
[6] Dept. of Mathematics, UBC, Vancouver

2 Background

During the manufacture of coated paper products, a paper-making stock consisting of water and 1% or less wood fibers is prepared by chemically or mechanically separating the fibers from wood. A screening process removes most of the water; the remainder is removed through pressing against felts and contact drying. The web is further densified by passing it through high pressure calender rolls, resulting in about a two-fold decrease in caliper of the pressed and dried paper. The web may then pass through a number of calender nips. The geometry for one such nip is shown in Fig. 1. This last stage of densification involves high temperatures and pressures that lead to high stresses in the roll material.

A stack consists of two rolls: one has a polymeric elastomer covering, the other is a solid iron alloy (the thermoroll). It is our task to estimate the stresses in the thermoroll under standard operating conditions, and determine whether it is possible, under certain conditions, for cracking or roll failure to occur.

3 A Detailed Description

The thermoroll consists of a hollow cylinder, rigidly attached at either end to a rotating bearing. It is hydraulically loaded to 350kN/m, leading to a deflection at its center of 1.6mm. The roll has inner and outer radii of 560 and 750mm, respectively. It contains 45 bore holes with radii 16mm. Oil, heated to a temperature of 253°C, flows through these boreholes at a rate of 33.7 L/s with an energy influx of approximately 800kW. As noted by Dr. Roman Popil, the temperature on the inner bores may be a little different from the oil temperature and is typically an unknown quantity. We label the bore temperature as T_{bore} in the analysis below. The typical configuration is shown in Fig. 1 and 2.

The thermoroll is made by a casting process such that the outer layer, the so-called 'chill", having cooled first upon contact with the walls of the mold, imparts a residual radial stress into the roll. The thermal and elastic properties of the chill are different from that of the bulk material.

The web enters the nip at a temperature of 66°C, typically traveling at 18m/sec. Its temperature, measured some distance from the nip, increases by approximately 26°C.

Periodically the polymer covered roll is washed, providing a source for dripping water. This may fall onto the iron roll and subsequently evaporate or 'jump" off the hot surface (and so have little effect on heat transfer).

A number of sources for stress build-up in this system are easily identified, for example:

- Large temperature gradients (and consequently thermal stresses) will occur in the vicinity of the nip.

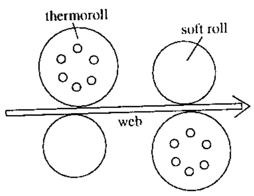

Figure 1: A sequence of thermorolls.

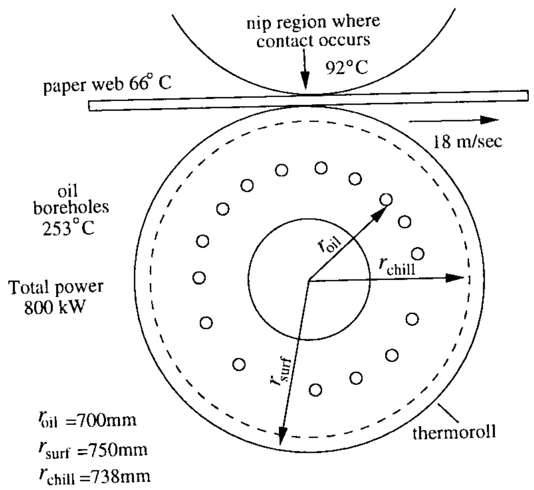

Figure 2: Schematic plot of geometry simplified.

- Cooling by dripping water may have a significant local effect.
- The iron roll manufacturing process will invariably lead to built-in stresses (estimated by the manufacturers to have compressive radial stress components of 150 MPa).
- Another compressive stress field, transmitted through the web, due to the roll's weight and loading.

The main questions for the study group to address are:

- What will be the total stress intensity (residual, thermal, loading ...) induced during this process?
- Are there conceivable operating conditions under which the stresses could become high enough to cause cracking, or even worse for catastrophic failure to occur?

The main focus of our group was to study the second question.

4 Physical Estimates

We first estimate whether the energy input from the oil boreholes and the quoted temperature difference across the roller are consistent. Specifically, we would like to estimate the surface temperature of the roller.

As will be shown in §4, the perturbing effect of the nip on the rapidly rotating drum is small except near the nip. Thus, we can approximate the temperature in the annular iron drum between the oil boreholes and the outer surface as the radial function

$$T(r) = A + B \ln r\,, \qquad r_{oil} < r < r_{surf}\,. \tag{1}$$

The values for r_{oil} and r_{surf} are given in Appendix A, and are $r_{oil} = 700$mm and $r_{surf} = 750$mm, respectively. The boundary condition $T = T_{bore}$ at $r = r_{oil}$ determines one relation between A and B while the other relation is found from the given total heat flux into the roller from the oil, which was quoted in §2. We estimate

$$\frac{dQ_{in}}{dt} = 2\pi r_{oil} \kappa T_r L_{roll} = P \quad \text{on} \quad r = r_{surf}\,. \tag{2}$$

Here P is the total heat flux and L_{roll} is the length of the roller. Using the data provided, and taking κ as that for iron, we estimate $B = 398°$C. This indicates a temperature difference between the borehole radius and the outer surface of

$$\triangle T = B \ln\left(r_{surf}/r_{oil}\right) = 28°\text{C}. \tag{3}$$

Using a more refined calculation, taking into account the different values of the thermal diffusivity κ for the chill and the core, we estimate a temperature difference of 32°C. In §5 below, we use the surface temperature of 192°C as measured by MacMillan Bloedel.

Next, we estimate the heat flux and temperature gradient in the roller surface just below the nip. With a specified nip width of 1.1cm and the heat flow to the web, the estimated radial heat flux ϕ is

$$\phi = 50\frac{\text{kW}}{\text{m}}/0.011\text{m} = 4.5 \times 10^6\ \text{W/m}^2\,. \tag{4}$$

Thus, since $\phi = \kappa T_r$ on the roller surface where κ is the thermal diffusivity of the chill, we get the estimated surface temperature gradient

$$T_r = O(10^5)\ °\text{C/m} = O(10^3)\ °\text{C/cm}\,. \tag{5}$$

This is much larger than the overall, or average, radial temperature gradient of 5°C/cm through the roll radius. Therefore, it is clear that we must do a careful analysis of the temperature gradients and the stress field near the nip. This is done below in §4 – §6.

Finally, we estimate the effect of water droplets. Water may be dripped onto the thermoroll when the paper web is interrupted in order to clean the top roller. The effect of these water droplets on the formation of micro-cracks seems very difficult to determine analytically. The goal would be to first calculate the temperature gradient on the surface of the roller just under the droplet. To do so we would need better observations of droplet size and lifetime. Apparently the manufacturer claims a droplet lifetime of the order of 1 second whereas MacMillan Bloedel has estimated the "Leidenfrost thermal flux lower limit" as input information.

We now consider a simple scenario. Suppose that we have a hemispherical droplet of radius a, where $a = 6.2$mm. The required latent heat to evaporate the droplet is $C_{lat} = 2.25610^6$J/kg. Thus, the estimate of the heat flux ϕ into the droplet across a small patch of roller surface under the droplet is

$$\phi = \frac{2\pi}{3t_{drop}} \left(\frac{a^3 \rho C_{lat}}{\pi a^2} \right) = \frac{2a\rho C_{lat}}{3t_{drop}} \,. \tag{6}$$

Using the estimates $a = 6.2$mm and the droplet lifetime $t_{drop} = 1$sec, we get an estimate $\phi = 10^7$W/m^2, which is four times larger than the heat flux estimated from the nip region. It therefore, appears crucial to do a careful analysis of temperature gradients and the resulting stress field near the droplet. This analysis is very difficult and was not done by our group.

5 The Global Temperature Field

In this section we calculate the temperature field in the region away from the nip to determine the effect of the oil bores on the heating of the drum. This is referred to as the **global problem**. In this problem, the nip region is replaced by a point sink of strength Q. The strength of this sink can be determined by the estimate obtained in §3.

It is convenient in the analysis to fix ourselves in a frame in which the thermoroll is stationary and the nip region on the edge of the thermoroll is rotating at an angular velocity $\omega = v/r_{surf}$. The mathematical model for the temperature field T, where T is measured in °C, is

$$T_t = \kappa \left(T_{rr} + r^{-1} T_r + r^{-2} T_{\theta\theta} \right), \quad r_{oil} < r < r_{surf}, 0 \leq \theta < 2\pi, \tag{7a}$$

$$T(r_{oil}, \theta, t) = T_{bore} \,, \tag{7b}$$

$$\kappa_{ch} T_r(r_{surf}, \theta, t) = Q\delta(\theta - \omega t) \,. \tag{7c}$$

Here k_{ch} is the thermal diffusivity of the chill and δ is the Dirac delta function. The parameter κ in (7a) is piecewise constant, with $\kappa = \kappa_{ch}$ in the chill region $r_{chill} < r < r_{surf}$, and $\kappa = \kappa_{co}$ in the core region $r_{oil} < r < r_{chill}$. The values for these constants are given in Appendix A. As a simplifying approximation to the geometry, in this model we have replaced the individual boreholes by a line of boreholes along $r = r_{oil}$. Although such an approximation should warrant further study, it greatly simplifies the analysis. In this model we have also assumed a negligible heat transfer between the air and the thermoroll. In a more refined analysis than is presented below, a Newtonian cooling boundary condition should be imposed on the edge of the thermoroll.

There are two goals to the analysis below. Firstly, we would like to justify why the temperature can be approximated by a radially symmetric function away from the nip region. Secondly, we would like to estimate the temperature gradient as we approach the nip region.

We introduce non-dimensional variables by $\rho = r/r_{surf}$ and $\tau = t/\omega$. The non-dimensional rotation rate ω_n is defined by

$$\omega_n = \omega r_{surf}^2/\kappa_{ch} \,. \tag{8}$$

We estimate that $\omega_n = 10^6$, which is very large. This value measures the importance of rotation as compared to thermal diffusion, and can be thought of as a Peclet number. The non-dimensional model is

$$\begin{aligned} \omega_n k^{-1} T_\tau &= T_{\rho\rho} + \rho^{-1} T_\rho + \rho^{-2} T_{\theta\theta} \,, \quad \rho_0 < \rho < 1 \,, \quad 0 \leq \theta < 2\pi \,, && \text{(9a)} \\ T(\rho_0, \theta, t) &= T_{bore} \,, && \text{(9b)} \\ T_\rho(1, \theta, t) &= \bar{Q}\delta(\theta - \tau) \,. && \text{(9c)} \end{aligned}$$

Here $\rho_0 \equiv r_{oil}/r_{surf}$, $\bar{Q} = Q r_{surf}/\kappa_{ch}$, while $k = 1$ in the chill region and $k = \kappa_{co}/\kappa_{ch}$ in the core. A schematic plot of the geometry is shown in Fig. 3.

We look for a solution to (9) in the form

$$T(\rho, \theta, t) = F(\rho, \phi) \qquad \text{where} \quad \phi = \theta - \tau \,. \tag{10}$$

The problem for $F(\rho, \phi)$ becomes

$$\begin{aligned} -\omega_n k^{-1} F_\phi &= F_{\rho\rho} + \rho^{-1} F_\rho + \rho^{-2} F_{\phi\phi} \,, \; \rho_0 < \rho < 1 \,, \; 0 \leq \phi < 2\pi && \text{(11a)} \\ F(\rho_0, \phi) &= T_{bore} && \text{(11b)} \\ F_\rho(1, \phi) &= \bar{Q}\delta(\phi) \,. && \text{(11c)} \end{aligned}$$

Next, we seek a solution to (11) in the rapid rotation limit $\omega_n \gg 1$. In the outer region, defined away from the nip near $\phi = 0$, we substitute the expansion

$$F(\rho, \phi) = F_0(\rho, \phi) + \frac{1}{\omega_n} F_1(\rho, \phi) + \cdots \,, \tag{12}$$

into (11) and collect powers of ω_n to obtain that

$$\begin{aligned} F_{0\phi} &= 0 \,, && \text{(13a)} \\ F_{0\rho\rho} + \rho^{-1} F_{0\rho} &= -k^{-1} F_{1\phi} \,, \quad \rho_0 < \rho < 1 \,. && \text{(13b)} \end{aligned}$$

Since F_1 is periodic in ϕ, it follows that $\int_{-\pi}^{\pi} F_{1\phi}\, d\phi = 0$. Therefore, upon integrating (13b), we obtain that F_0 satisfies

$$F_0 = A + B \ln \rho \,. \tag{14}$$

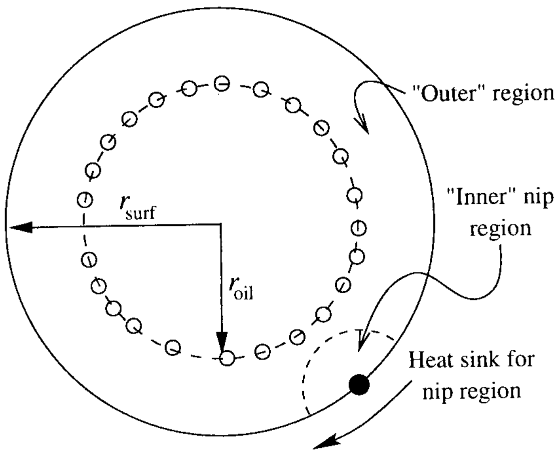

Figure 3: A heat sink is rotating on the boundary of the thermoroll.

One boundary condition for F_0 is $F_0 = T_{bore}$ at $\rho = \rho_0$. There are two possible conditions that can be imposed for the second relation. One choice would be to specify the flux out of $\rho = \rho_0$ as in §3, which would determine B. The second choice would be to satisfy the boundary condition $F_{0\rho} = 0$. Note that a better approximation to the boundary condition would be to impose a Newtonian cooling condition on the surface of the roller characterized by some Biot number, representing a heat transfer coefficient between the air and the chill. Specifying the flux out of the boreholes would enable us to calculate this coefficient. The temperature field, away from the nip region, is obtained by substituting (14) in (10).

Our first conclusion is that in the limit of rapid rotation the temperature field away from a thin zone near the nip region is radially symmetric.

The solution (14) is not valid in the vicinity of the nip region where $\phi = 0$. Thus, as is usual in singular perturbation problems, we must construct an inner solution near $\phi = 0$, $\rho = 1$. The extent of this region is $O(\omega_n^{-1})$. We introduce the local variables $\hat{\rho}$ and $\hat{\phi}$ by

$$\hat{\rho} = (1-\rho)\omega_n\,, \qquad \hat{\phi} = \phi\omega_n^{-1}\,. \tag{15}$$

The corresponding problem for F becomes

$$\begin{aligned} -F_{\hat{\phi}} &= F_{\hat{\rho}\hat{\rho}} + F_{\hat{\phi}\hat{\phi}}\,, \quad 0 < \hat{\rho} < \infty\,, \quad -\infty \le \hat{\phi} < \infty\,, && (16a)\\ F_{\hat{\rho}}(0,\hat{\phi}) &= \bar{Q}\delta(\hat{\phi})\,, && (16b)\\ F &\to 192 \quad \text{as} \quad \hat{\rho} \to \infty\,. && (16c) \end{aligned}$$

We have used the surface temperature of 192°C quoted by MacMillan Bloedel Research as the far field condition. A plot of the geometry is shown in Fig. 4.

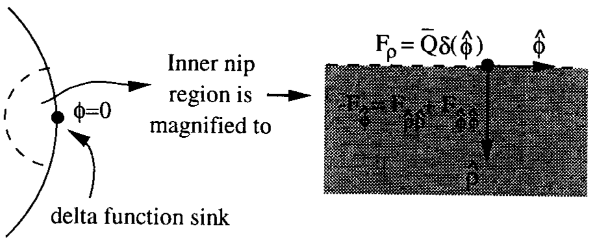

Figure 4:

The solution to this problem is readily found to be

$$F(\hat{\rho}, \hat{\phi}) = -\bar{Q}e^{-\hat{\phi}/2}K_0\left(\frac{1}{2}(\hat{\phi}^2 + \hat{\rho}^2)\right) + 192\,. \tag{17}$$

Here $K_0(z)$ is the modified Bessel function of the first kind of order zero. In terms of the original variables, we have

$$T(r, \theta, t) = 192 + \bar{Q}e^{-\omega_n(\theta - \omega t)}K_0\left(\frac{\omega_n}{2}\left[(1 - r/r_{surf})^2 + (\theta - \omega t)^2\right]^{1/2}\right)\,. \tag{18}$$

Therefore, using the asymptotic behavior of $K_0(z)$, we observe that as we approach the nip region the change in temperature $\Delta T = T - 192$ behaves logarithmically like

$$\Delta T \sim \frac{\bar{Q}}{2}\ln\left[(1 - r/r_{surf})^2 + (\theta - \omega t)^2\right]\,, \qquad \text{as} \quad r \to r_{surf}\,, \quad \theta \to \omega t\,. \tag{19}$$

Here $\bar{Q}$ is the strength of the heat sink. Thus, for the global problem the temperature decrease as we approach the nip region is only logarithmic with the distance from the nip. The effect of the resulting temperature gradient on the stress field is estimated in §6.

6 The Local Temperature Field

We now calculate the temperature field in the region near the nip. This is referred to as the **local problem**. In the near-nip region, the geometry is approximately planar as shown in Fig. 5. The contact region between the paper and the roller is approximately 2cm as shown in this figure. The goal is to estimate the temperature gradients near the **leading edge** where the paper first comes into contact with the roller (see the figure). It is in this region that we expect the temperature gradients to be largest. Note that the calculations below are done in a frame for which the leading edge is located at $X = 0$ (see Fig. 5).

From the data given in Appendix A, the values for the thermal diffusivity of the water κ_w, the chill κ_{ch} and the core κ_{co} are

$$\kappa_w = 0018\,\text{cm}^2/\text{sec}\,, \qquad \kappa_{ch} = .071\,\text{cm}^2/\text{sec}\,, \qquad \kappa_{co} = .143\,\text{cm}^2/\text{sec}\,. \tag{20}$$

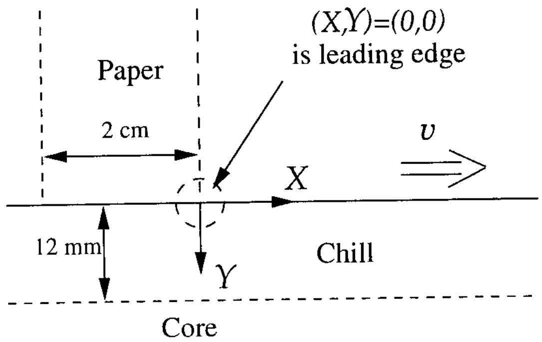

Figure 5: Schematic plot of contact region.

From these values, we can estimate a Peclet number, which is a dimensionless parameter giving a measure of the relative strengths of convection compared to the thermal diffusion. Since $\text{Pe} = vL/\kappa$, we can estimate a Peclet number using $v = 18\text{m/sec}$, $L = 2\text{cm}$, and $\kappa = 0.1\text{cm}^2/\text{sec}$ to get $\text{Pe} = 18000$, which is very large. Hence the temperature field near the nip is dominated by convection.

We now formulate the model. We approximate the temperature field in the near nip region using a steady-state convection-diffusion equation

$$-vT_X = \kappa\,(T_{XX} + T_{YY})\;, \tag{21}$$

where κ is piecewise constant. We then introduce non-dimensional variables by

$$x = X\text{Pe}/L\,, \qquad y = Y\text{Pe}/L\,, \tag{22}$$

where we take $L = 2\text{cm}$ and $\text{Pe} = vL/\kappa_{ch}$. In terms of these variables, the length of the contact region between the paper and the roller is extremely large and thus, as a good approximation, we take the contact region to be of semi-infinite extent occupying the region $x < 0,\ y = 0$. In terms of these new variables, the chill region extends very deeply below the contact region and hence we will take the chill to occupy the region below the x-axis.

We now formulate the boundary conditions. The line $x > 0,\ y = 0$ is where the roller is exposed to the air and hence we assume that there is negligible heat transfer between these two media (i.e. $T_y = 0$ for $x > 0,\ y = 0$). This assumption should be examined more carefully in a more refined analysis. In addition, we assume that the temperature field and the heat flux are continuous across the contact region.

Next, we give far field conditions for the temperature field. The surface temperature of the roller obtained from the global problem is estimated by MacMillan Bloedel Research to be $T = 192°\text{C}$. This yields the asymptotic matching condition $T \to 192°\text{C}$ as $y \to -\infty$. Finally, the web temperature into the nip is $66°\text{C}$ and thus we set $T \to 66°\text{C}$ as $y \to +\infty$.

To summarize, the model for the temperature field in the near nip region (see Fig. 6), where T is measured in °C is

$$-T_{+x} = \delta\,(T_{+xx} + T_{+yy}) \qquad y > 0\,, \quad -\infty < x < \infty\,, \tag{23a}$$

$$-T_{-x} = T_{-xx} + T_{-yy} \qquad y < 0\,, \quad -\infty < x < \infty\,, \tag{23b}$$

$$T_{+y}(x,0) = T_{-y}(x,0) = 0 \quad \text{for} \quad x > 0 \tag{23c}$$

$$T_{+}(x,0) = T_{-}(x,0)\,; \qquad \delta T_{+y}(x,0) = T_{-y}(x,0) \quad \text{for} \quad x < 0\,, \tag{23d}$$

$$T_{+} \rightarrow 66 \quad \text{as} \quad y \rightarrow +\infty\,; \qquad T_{-} \rightarrow 192 \quad \text{as} \quad y \rightarrow -\infty\,. \tag{23e}$$

Here T_+ and T_- are the temperature fields in the web and the chill regions, respectively. The small parameter δ is the ratio of the thermal diffusivities of the web and the chill,

$$\delta = \kappa_w / \kappa_{ch} \approx 1/40\,. \tag{24}$$

The goal is to calculate the temperature gradient near the leading edge $(x, y) = (0,0)$ and to determine its singular behavior. In particular, we calculate

$$I(x) \equiv T_{-y}(x, 0^-) \quad \text{as} \quad x \rightarrow 0^-\,. \tag{25}$$

The problem (23) is difficult to solve analytically and hence we will seek an asymptotic solution valid for small δ (i.e. $\delta \ll 1$). When δ is small, the extent of diffusion of heat from the roller into the web is limited, and hence the temperature in the chill region deviates only slightly from its asymptotic value as $y \rightarrow -\infty$. In addition, a thermal boundary layer occurs in the web region near $y = 0$ and it has a width $O(\delta^{1/2})$. The relevant asymptotic expansion for T_+ is

$$T_+(x, \tilde{y}\delta^{1/2}) \equiv u(x, \tilde{y}) = u_0(x, \tilde{y}) + O(\delta)\,, \tag{26}$$

while for T_- it is

$$T_-(x, y) = 192 + \delta^{1/2} v(x, y) + \cdots\,. \tag{27}$$

Substituting (26) and (27) into (23), and collecting powers of δ, we find that u_0 satisfies

$$-u_{0x} = u_{0\tilde{y}\tilde{y}} \qquad y > 0\,, \tag{28a}$$

$$u_{0\tilde{y}}(x,0) = 0 \quad \text{for} \quad x > 0\,; \qquad u_0(x,0) = 192 \quad \text{for} \quad x < 0\,, \tag{28b}$$

$$u_0 \rightarrow 66 \quad \text{as} \quad y \rightarrow +\infty\,. \tag{28c}$$

In terms of this solution, the correction v to the temperature in the thermoroll satisfies

$$-v_x = v_{xx} + v_{yy} \qquad y < 0\,, \quad -\infty < x < \infty\,, \tag{29a}$$

$$v_y(x,0) = 0 \quad \text{for} \quad x > 0\,; \qquad v_y(x,0) = u_{0\tilde{y}}(x,0) \quad \text{for} \quad x < 0\,. \tag{29b}$$

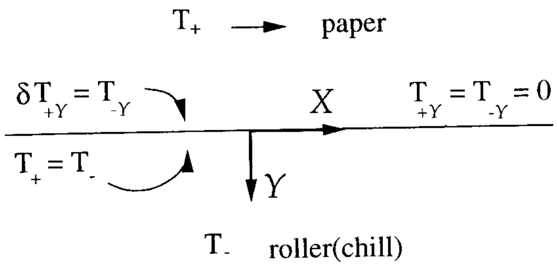

Figure 6:

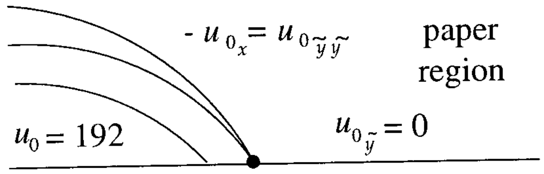

Figure 7: Sketch of u_0 isotherms.

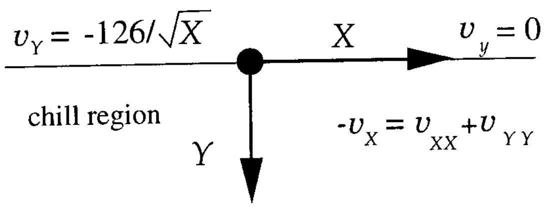

Figure 8:

To get a well-posed problem, we solve (28) in the region $x < 0$, with the "initial" condition $u_0(0, \tilde{y}) = 192$. The solution is readily found to be

$$u_0(x, \tilde{y}) = 66 + 126 \text{ Erfc}\left(\tilde{y}/2(-x)^{1/2}\right) , \tag{30}$$

where Erfc(z) is the complementary error function. Thus, the isotherms occur along the curves $\tilde{y} = c(-x)^{1/2}$ for $c > 0$ and $x < 0$ (see Fig. 7). A simple calculation then yields

$$u_{0\tilde{y}}(x, 0) = -\frac{126}{(-\pi x)^{1/2}} , \quad \text{for} \quad x < 0 , \tag{31}$$

which is used in (29) (see Fig. 8).

The solution to (29) can be found in terms of the Green's function, $G(\mathbf{x}'; \mathbf{x})$, which solves the adjoint problem corresponding to the convection-diffusion operator in (29)

$$\begin{aligned} G_{x'x'} + G_{y'y'} - G_{x'} &= \delta(\mathbf{x}' - \mathbf{x}) , \quad y' < 0 , \quad -\infty < x' < \infty , & \text{(32a)} \\ G_{y'} &= 0 \quad \text{on} \quad y' = 0 . & \text{(32b)} \end{aligned}$$

π

The solution to (32), found from the method of images, is

$$G(\mathbf{x}';\mathbf{x}) = -\frac{1}{2\pi}e^{(x'-x)/2}\left[K_0\left(|\mathbf{x}'-\mathbf{x}|\right) + K_0\left(|\mathbf{x}'-\mathbf{x}^*|\right)\right]. \tag{33}$$

where $\mathbf{x} = (x, y)$, $\mathbf{x}' = (x', y')$, and $\mathbf{x}^* = (x, -y)$. This yields the integral representation

$$v(x,y) = -\frac{132}{\sqrt{\pi}}\int_{-\infty}^{\infty}\frac{1}{\sqrt{-x'}}G(\mathbf{x}';\mathbf{x})\big|_{y'=0}\,dx'. \tag{34}$$

Substituting (30) and (34) into (26) and (27) yields the temperature profile in the web and the chill regions, respectively. It is easy to show that the limiting behavior of v as we approach the leading edge is

$$v \sim Cr^{1/2}\sin\theta/2\,, \quad \text{as} \quad r = |\mathbf{x}| \;\rightarrow\; 0\,, \tag{35}$$

where $C = -252/\sqrt{\pi}$.

The solution for T_- in the paper becomes invalid in an $O(\delta)$ neighborhood of leading edge. This follows from the fact that we have neglected the diffusion term T_{-xx} in obtaining (28). Hence we need an inner-inner region where $x = O(\delta)$ and $y = O(\delta)$. Introduce the new variables

$$\hat{x} = x/\delta\,, \qquad \hat{y} = y/\delta\,, \tag{36}$$

and expand

$$T_+ = \hat{u}(\hat{x},\hat{y}) + \cdots\,, \qquad T_+ = 192 + \delta\hat{v}(\hat{x},\hat{y}) + \cdots. \tag{37}$$

Substituting (36) and (37) into (23), we obtain that $\hat{u}$ satisfies

$$-\hat{u}_{\hat{x}} = \hat{u}_{\hat{x}\hat{x}} + \hat{v}_{\hat{y}\hat{y}} \qquad \hat{y} > 0\,, \tag{38a}$$

$$\hat{u}_{\hat{y}}(\hat{x},0) = 0 \quad \text{for} \quad \hat{x} > 0\,; \qquad \hat{u}(\hat{x},0) = 192 \quad \text{for} \quad \hat{x} < 0\,, \tag{38b}$$

$$\hat{u} \rightarrow 66 \quad \text{as} \quad \hat{y} \rightarrow +\infty\,. \tag{38c}$$

In terms of the solution to this problem, $\hat{v}$ satisfies

$$\hat{v}_{\hat{x}\hat{x}} + \hat{v}_{\hat{y}\hat{y}} = 0 \qquad \hat{y} < 0\,, \quad -\infty < \hat{x} < \infty\,, \tag{39a}$$

$$\hat{v}_{\hat{y}}(\hat{x},0) = 0 \quad \text{for} \quad \hat{x} > 0\,; \qquad \hat{v}_{\hat{y}}(\hat{x},0) = \hat{u}_{\hat{y}}(\hat{x},0) \quad \text{for } \hat{x} < 0 \tag{39b}$$

The solution $\hat{v}$ must match with the behavior (35) in the far field.

The solution to (38) can be found explicitly in terms of the parabolic coordinates ξ and η defined by

$$\hat{x} = \frac{1}{2}(\xi^2 - \eta^2)\,, \qquad \hat{y} = \xi\eta\,. \tag{40}$$

In terms of these coordinates the problem (38) reduces to the following ordinary differential equation problem for $\hat{u}(\eta)$:

$$\hat{u}_{\eta\eta} + \eta\hat{u}_\eta = 0\,, \quad 0 < \eta < \infty\,; \qquad \hat{u}(0) = 192\,, \quad \hat{u}(\infty) = 66\,. \tag{41}$$

The solution to this problem is

$$\hat{u}(\eta) = 66 + 126\ \mathrm{Erfc}\,(\eta/2)\,. \tag{42}$$

Using the definition of the change of coordinates we can calculate the derivative needed in the problem (39) for $\hat{v}$. We get

$$\hat{u}(\hat{x}, 0) = -\frac{126}{(-\pi x)^{1/2}}\,, \quad \text{for} \quad x < 0\,, \tag{43}$$

Finally, we can substitute (43) into (39) and solve the resulting problem for $\hat{v}$ to get

$$\hat{v} = C\hat{r}^{1/2}\sin(\theta/2)\,, \qquad \text{where} \quad C = -252/\sqrt{\pi} \qquad \text{and} \quad \hat{r} = \left(\hat{x}^2 + \hat{y}^2\right)^{1/2}\,. \tag{44}$$

Substituting (44) into (37) determines the temperature field in the chill region of the thermoroll in the immediate vicinity of the leading edge where the paper first makes contact with the roller.

The main conclusion from this analysis is that this temperature field near the leading edge has the behavior

$$T_- \sim Br^{1/2}\sin(\theta/2) \qquad \text{as} \quad r \to 0\,, \tag{45}$$

for some constant B. Thus, it has an infinite gradient of square-root type at the leading edge. In §6 we estimate whether this singular form leads to a singular stress field at the leading edge.

7 The Stress Field

We now estimate the stress field induced by the temperature gradients calculated in §4 and §5. We will consider both the local and the global problems.

The equilibrium equation from elasticity theory for the displacement vector $\mathbf{u}$ is

$$\frac{3(1-\nu)}{(1+\nu)}\nabla\left(\nabla\cdot\mathbf{u}\right) - \frac{3(1-2\nu)}{2(1+\nu)}\nabla\times\nabla\times\mathbf{u} = \alpha\nabla T\,. \tag{46}$$

Here ν is Poisson's ratio, $\alpha\nabla T$ is the body force induced by the thermal gradient, and α is a constant. The stress tensor σ_{ij} is determined in terms of $\mathbf{u}$ by

$$\sigma_{ij} = \lambda\delta_{ij}\frac{\partial u_k}{\partial x_k} + G\left(\frac{\partial u_i}{\partial x_j} + \frac{\partial u_j}{\partial x_i}\right)\,. \tag{47}$$

Here λ and G are the Lame' constants. Thus, the stress is (essentially) proportional to the first derivatives of $\mathbf{u}$.

Consider the **local problem** for which the temperature field behaves like (45) at the leading edge. Then decomposing $\nabla\mathbf{u}$ in terms of a radial component u_r and an angular component u_θ, we get the following equations from (46):

$$\frac{3(1-\nu)}{(1+\nu)}\left(\partial_{rr}u_r+\cdots\right)-\frac{3(1-2\nu)}{2(1+\nu)}\left(\frac{\partial_{r\theta}u_\theta}{r}+\cdots\right)=\alpha\left(\frac{C}{2r^{\frac{1}{2}}}\right)\sin\left(\frac{\theta}{2}\right), \tag{48a}$$

$$\frac{3(1-\nu)}{(1+\nu)}\left(\frac{\partial_{r\theta}u_r}{r}+\cdots\right)+\frac{3(1-2\nu)}{2(1+\nu)}\left(\partial_{rr}u_\theta+\cdots\right)=-\alpha\left(\frac{C}{2r^{\frac{1}{2}}}\right)\cos\left(\frac{\theta}{2}\right). \tag{48b}$$

From these equations, a simple dominant balance argument shows that the two components satisfy $u_r = O(r^{3/2})$ and $u_\theta = O(r^{3/2})$ as $r \to 0$. Thus the stress field has the form

$$\sigma_{ij} = O\left(r^{\frac{1}{2}}\right) \qquad \text{as} \quad r \to 0. \tag{49}$$

Hence the stress field is not singular at the leading edge, and there is no significant stress intensification, such as that determined by a stress intensity factor. In fact, the stress field behaves like that for a contact problem (i.e. a Barenblatt "crack").

Now consider the **global problem** where the nip region is approximated by a delta function. The geometry is shown in Fig. 4 and the temperature field has the behavior given in (19). Substituting $T \sim \ln r$ into (46) we can obtain the behavior of u_r using a dominant balance argument. We estimate $\partial_r u_r = O(\ln r)$ and hence the radial component of the stress is $\sigma_r = O(\ln r)$. Thus, the stress field grows logarithmically in the outer region but is then cut off as we approach the inner-inner region. Once again, we conclude that there is no significant intensification of the stress, such as that determined by a square root singularity for which a stress intensity factor can be defined.

8 Conclusions

The main focus of our group was to calculate the temperature gradient in the thermoroll and to determine whether this gradient can lead to an intensification of stress in the nip region.

The temperature gradient was calculated for both a global temperature model in which the nip is represented by a point source and a local temperature problem, defined in the vicinity of the nip region, where we studied in detail the region where the paper first comes into contact with the roller. For both the local and global temperature problems we calculated the singular behavior of the thermal field. In §6, we used the singular behavior of the thermal field in a model to estimate the stress field for both the local and global problems. The goal was to ascertain whether such a temperature gradient can lead to a singular stress field. Such a stress field is known in other circumstances to induce crack formation. Our conclusion in §6 is that the stress field is not singular for either the local or global problems, and hence, from our model of the thermoroll, the temperature gradients are not likely to be the cause of roll fracture.

We also showed that in the limit of large drum rotation, which is the usual operating regime of the thermoroll, the temperature distribution inside the thermoroll is well approximated by a radially symmetric function. This can allow for an accurate calculation of the surface temperature on the roller once a more precise boundary condition can be applied to the roller surface.

Finally, a crude physical estimate in §3 suggested that there can be extremely large temperature gradients as a result of dripping water onto the thermoroll. This problem certainly warrants an intensive investigation.

1 Acknowledgements:

We are grateful to Dr. Roman Popil of MacMillan Bloedel Research Ltd. for his explanation of this problem to us and for his detailed comments on this report. We would also like to thank Dhavide Aruliah for preparing the figures for this paper.

2 Appendix A: Physical Constants

We summarize some relevant physical constants given by MacMillan Bloedel Research:

Web temperature out of nip	= 92°C
Web temperature into nip	= 66°C
Web velocity	= 18m/sec
Web width	= 7770 mm
Inner core radius	= 560mm
Outer core radius	= 750mm
Thickness of chill	= 12mm
Thickness of shell	= 49mm
Thermal conduct. chill	= 24W/mK
Thermal conduct. core	= 48W/mK
Bore hole radius	= 16mm
Number of bores	= 45
Oil flow rate	= 33.7L/sec
Oil temperature	= 253°C

The thermal diffusivities of the water, chill and core, which we label by κ_w, κ_{ch} and κ_{co}, respectively, are now calculated in terms of more conventional units. For water, $\rho = 10^3\,\text{kg/m}^3$, $C_\rho = 4186\,\text{J/kg-K}$, $k = 0.6\,\text{W/mK}$, and thus

$$\kappa_w = k/\rho C_\rho = 0.142 \times 10^{-6}\,\text{m}^2/\text{sec} = 0.142 \times 10^{-2}\text{cm}^2/\text{sec}\,. \tag{50}$$

For the chill, $\rho = 8.0 \times 10^3\,\mathrm{kg/m^3}$, $C_\rho = 420\,\mathrm{J/kg\text{-}K}$, $k = 24\,\mathrm{W/mK}$, and thus

$$\kappa_{ch} = k/\rho C_\rho = 0.71 \times 10^{-5}\,\mathrm{m^2/sec} = 0.071\mathrm{cm^2/sec}\,. \tag{51}$$

Lastly, $\kappa_{co} = 2\kappa_{ch}$.

Finally, we quote the estimate of the heat flow into the web given by Macmillan Bloedel Research. For each unit length along the roll we have $dm/dt = 1.1\mathrm{kg/s}$ and the heat flux into the web is

$$\frac{dQ}{dt} = \sum C_\rho \frac{dm}{dt} \triangle T = 50\mathrm{kW}\,. \tag{52}$$

Here $\triangle T = 26°\mathrm{C}$ is the temperature difference along the web. This input estimate might be based on too much water content, and if so it would turn out that the heat input into the web is smaller by a factor of ten.